

# **Addendum: 3D Geomechanical Model for Gas Storage Bergermeer for extension of the working pressure from 133 to 150 bar**

**Report for TAQA Energy BV**

Prepared by

Fenix Consulting Delft BV

Date

April 2018

# **Addendum: 3D Geomechanical Model for Gas Storage Bergermeer for extension of the working pressure from 133 to 150 bar**

Report for TAQA Energy BV

Date  
April 2018

## **DISCLAIMER**

Fenix Consulting Delft nor any person acting on behalf of Fenix:

- Makes any warranty or representation, express or implied, with respect to the accuracy, completeness, or usefulness of the information contained in this report, or that the use of any apparatus, method, or process disclosed in this report may not infringe privately owned rights; or
- Assumes any liability with respect to the use of, or for damages resulting from the use of, any information, apparatus, method, or process disclosed in this report.

## Nederlandse samenvatting

Dit rapport bevat een geomechanische evaluatie van gasopslag-operaties in het Bergermeer reservoir met het doel om het seismische risico in kaart te brengen als gevolg van een drukverhoging van de maximale reservoirdruk van 133 naar 150 bar. Dit rapport betreft een uitbreiding van het rapport “3D Geomechanical Model for Gas Storage Bergermeer” welke gericht was op drukwisselingen tussen 77 en 133 bar.

Omdat de micro-seismische activiteit in de operationele fase van de gasopslag duidelijk is afgenomen, is het waarschijnlijk dat een verdere drukverhoging gedaan kan worden zonder het veroorzaken van sterke bevingen.

Het geomechanisch model laat ook zien dat verhoging van de maximale druk van 133 naar 150 bar een verwaarloosbare invloed heeft op het seismisch risico, omdat de kritische spanning op de centrale breuk ongevoelig is voor de drukverhoging terwijl de zeer lage activiteit op de Oostbreuk alleen van de druksnelheid afhangt en niet van het drukk niveau.

### Conclusies 150 bar opslag cycli

- Toename van de maximale werkdruk van 133 naar 150 bar heeft een verwaarloosbare invloed op het seismisch risico:
  - Voor de gehele centrale breuk wordt seismisch risico bepaald door de lage druk kant van de cyclus, dus wordt de gemiddelde kritische spanning op de breuk niet beïnvloed door verhoging van de werkdruk.
  - Het meest kritisch gespannen deel van de centrale breuk wordt instabiel bij hogere druk, maar dit effect vlakt af bij hogere druk en dus veroorzaakt de hogere werkdruk tussen 133 bar en 150 bar geen hogere seismiciteit.
  - Het verhogen van de maximum werkdruk naar 150 bar geeft dus geen verhoging van het seismisch risico voor de centrale breuk vergeleken met de opslag cycli met een maximum werkdruk van 133 bar.
  - De micro-seismiciteit op de Oost breuk wordt bepaald door de druksnelheid. Omdat de druksnelheid hetzelfde is bij hogere drukken, zal de verwachte seismiciteit ook niet toenemen bij een hogere werkdruk op de Oost breuk.
- De amplitude van de bodembeweging blijft bij een 77-150 bar cyclus binnen de 1 cm.

## Executive Summary

This report contains a geomechanical evaluation of the Bergermeer storage reservoir response to gas operations with the aim to determine the seismic risk from increasing the maximum reservoir pressure from 133 to 150 bar. This addendum concerns a direct extension of the report “3D Geomechanical Model for Gas Storage Bergermeer” that focused on forecast cycles in the pressure range 77-133bar.

Since micro-seismic activity during the operational phase of the gas storage has clearly declined, it is likely that further pressure increase can be done safely, without inducing strong seismic events.

The Geomechanical model also shows that increasing the maximum operating pressure from 133 to 150 bar has negligible influence on seismic risk because the critical stress at the Midfield fault is insensitive to higher pressure and the very weak activity on the East fault only depends on rate of pressure increase and not on the pressure level.

### Conclusions for 150 bar storage cycles

- Increasing the working pressure from 133 bar to 150 bar has negligible influence on seismic risk:
  - For the entire Midfield fault, seismic risk is determined by the lower pressure bound of the storage cycles. So, the average critical stress ratio is not affected by the higher working pressure.
  - The most critical patch on the Midfield fault is most unstable at high pressure but the critical stress ratio is about the same for 150 bar compared with 133 bar, because it levels off at higher pressure.
  - Therefore, increasing the working pressure to 150 bar does not increase the seismic risk for the Midfield fault compared with storage cycles with maximum pressure of 133 bar.
  - The micro-seismicity rate at the East fault is determined by pressure rate. Since the rate is the same for higher working pressure, the expected seismic rate will not increase for higher working pressure at the East fault.
- The amplitude of the surface movement remains less than 1cm during a 77-150 bar storage cycle.

# Contents

<b>NEDERLANDSE SAMENVATTING .....</b>	<b>III</b>
<b>EXECUTIVE SUMMARY .....</b>	<b>IV</b>
Contents.....	v
List of Figures .....	vi
Nomenclature .....	vi
<b>1 INTRODUCTION.....</b>	<b>1</b>
<b>2 PRESSURE RESPONSE.....</b>	<b>1</b>
<b>3 STRESS SIMULATION FOR 77-150 BAR FORECAST CYCLES .....</b>	<b>1</b>
<b>4 SUBSIDENCE AND HEAVE FOR FORECAST CYCLES.....</b>	<b>5</b>
<b>5 DISCUSSION.....</b>	<b>6</b>

## List of Figures

- Figure 1: Bulk Volume average block pressure versus gas block pressure in the gas bearing blocks (left) 77-133 bar forecast cycles and (middle) 77-150 bar forecast cycles. (Right) figure shows the bulk volume average reservoir pressure and gas pressure in time for both forecasts. ....1
- Figure 2: Contours of critical stress ratio on the Midfield fault, at the start of refill. The black lines indicate the reservoir blocks (solid for Eastern side and dashed for Western side). The red line is the maximum critically stressed area during depletion on which the stress is computed to determine how close the fault is to inducing large earthquakes. ....2
- Figure 3: Contours of critical stress ratio on the Midfield fault, just before the time of the largest micro-seismic event. The only critically stressed patches occur at the boundaries of the maximum slippage area. ....2
- Figure 4: MC plot of selected points on the fault, shown in Figure 3. (left) 77-133 bar cycles (right) 77-150 bar cycles. Note that the points are chosen at slightly different position (77-133 vs 77-150 bar), this results in slightly different stress paths. However the overall trend is the same (see text). ....3
- Figure 5: Normal stress, shear stress and critical stress ratio for point 1 (see Figure 3) vs. time. The critical stress ratio at this peaks at high average reservoir pressure, due to the additional shear stress from the depletion earthquakes. (left) 77-133 bar cycles (right) 77-150 bar cycles. ....3
- Figure 6: Magnitude from slip for the Midfield fault with average gas pressure and observed micro-seismic rate (upper graphs) for (left) the 133 bar case (right) the 150 bar case. Rate is defined as events per 3 months times 0.1. The lower graphs show the average critical stress ratio. This ratio remains below the level of the maximum recorded historical micro-seismic event of magnitude 1. ....4
- Figure 7: Micro-seismic rate and predicted rate that is derived from the shear stress rate and the stress level on the fault. Rate is defined as event per 3 months times 0.1. The predicted rate was calibrated on the absence of micro-seismicity after 2014. Refill, storage and (left) 77-133 bar forecast cycles and (right) 77-150 bar forecast cycles. ....4
- Figure 8: Magnitude from potential slip for the Midfield fault with average gas pressure and observed micro-seismic rate (upper graphs) for (left) the 133 bar case (right) the 150 bar case with friction coefficient 0.65. Rate is defined as event per 3 months times 0.1. In this case, no slip was applied, so the critically stressed region persists. The maximum magnitude of 2.2 that is predicted for this worst case is the same as the maximum magnitude for 133 bar maximum pressure. The lower graphs show the average critical stress ratio. ....4
- Figure 9: Magnitude from slip for the East fault with average gas pressure and observed micro-seismic rate (upper graphs) for (left) 77-133 bar case and (right) 77-150 bar case. Rate is defined as events per 3 months. The lower graphs show the average critical stress ratio. During the storage cycles the ratio remains below the level of the maximum recorded historical micro-seismic event in 2011. ....5
- Figure 10: Micro-seismic rate and predicted rate that is derived from the shear stress rate on the fault. Rate is defined as events per 3 months. (left) 77-133 bar cycles and (right) 77-150 bar cycles. ....5
- Figure 11: Response heave of the 4 observation stations and the maximum heave during the historical storage and forecast simulations (2014-2021) plotted against the gas pressure. (left) 77-133 bar forecast cycles and (right) 77-150 bar forecast cycles. The squares are a Kelvin-Voigt fit of the FEM results for which the corresponding relaxation time are shown. ....6

## Nomenclature

Units: SI (m= metre, s= second, kPa =10<sup>3</sup>Pa, MPa =10<sup>6</sup>Pa, GPa =10<sup>9</sup>Pa)

Dimensions: m= mass, L= length, t= time

Variable	Description	Units	Dimensions
----------	-------------	-------	------------

$A_p$	:	Poroelastic coefficient	[-]	(-)
$A$	:	Area	[m <sup>2</sup> ]	(L <sup>2</sup> )
$c$	:	cohesion	[MPa]	(m/Lt <sup>2</sup> )
$c_g$	:	grain compressibility	[1/MPa]	(Lt <sup>2</sup> /m)
$c_r$	:	rock compressibility	[1/MPa]	(Lt <sup>2</sup> /m)
$c_m$	:	compaction coefficient	[1/MPa]	(Lt <sup>2</sup> /m)
$E$	:	Young's modulus	[GPa]	(m/Lt <sup>2</sup> )
$E_{eff}$	:	Effective Young's modulus	[GPa]	(m/Lt <sup>2</sup> )
$\tilde{E}$	:	elastic coefficient	[Pa/m]	(m/L <sup>2</sup> t <sup>2</sup> )
$G, G_{EL}$	:	Shear modulus	[GPa]	(m/Lt <sup>2</sup> )
$G_\infty$	:	Relaxed shear modulus at infinite time	[GPa]	(m/Lt <sup>2</sup> )
$g$	:	Stress gradient	[kPa/m]	(m/L <sup>2</sup> t <sup>2</sup> )
$H$	:	Height	[m]	(L)
$L_z$	:	Characteristic height	[m]	(L)
$K_h$	:	horizontal stress ratio	[-]	(-)
$M_0$	:	seismic moment	[N m]	(mL <sup>2</sup> /t <sup>2</sup> )
$M_c$	:	compaction moment	[N m]	(mL <sup>2</sup> /t <sup>2</sup> )
$M_w$	:	moment magnitude	[-]	(-)
$p$	:	pressure	[MPa]	(m/Lt <sup>2</sup> )
$p(N,t)$	:	poisson distribution	[-]	(-)
$t$	:	time	[s]	(t)
$u, v, w$	:	displacement	[m]	(L)
$\mathbf{u}$	:	displacement vector	[m]	(L)
$u_{dip}$	:	displacement in dip direction	[m]	(L)
$u_{strike}$	:	displacement in strike direction	[m]	(L)
$V_{res}$	:	reservoir volume	[m <sup>3</sup> ]	(L <sup>3</sup> )
$\alpha_B$	:	Biot coefficient	[-]	(-)
$\varepsilon$	:	strain	[-]	(-)
$\varepsilon_T$	:	volumetric strain	[-]	(-)
$\in_k$	:	average deviation in surface heave of station k	[m]	(L)
$\in$	:	average deviation in surface heave	[m]	(L)
$\varepsilon$	:	strain	[-]	(-)
$\nu$	:	Poisson's ratio	[-]	(-)
$\eta$	:	viscosity	[Pa s]	(m/L t)
$\mu$	:	friction coefficient	[-]	(-)
$\sigma_d$	:	deviatoric stress	[MPa]	(m/Lt <sup>2</sup> )
$\sigma_{H,max}$	:	maximum horizontal stress	[MPa]	(m/Lt <sup>2</sup> )
$\sigma_{H,min}$	:	minimum horizontal stress	[MPa]	(m/Lt <sup>2</sup> )
$\sigma_{vert}$	:	vertical stress	[MPa]	(m/Lt <sup>2</sup> )
$\sigma_n$	:	normal stress on fault plane	[MPa]	(m/Lt <sup>2</sup> )
$\tau$	:	shear stress	[MPa]	(m/Lt <sup>2</sup> )
$\tau_i$	:	relaxation time	[s]	(t)





# 1 Introduction

This addendum investigates the seismic risk and surface heave by extension of the working pressure in the forecast cycles from 77-133 bar to 77-150 bar in Gas Storage Bergermeer. For detailed analysis, model construction and calibration of the underlying Geomechanical model see the report “3D Geomechanical Model for Gas Storage Bergermeer”. Here only the differences are considered.

## 2 Pressure Response

Figure 1 compares the pressure in the forecast cycles with swing from 77-150 bar to the forecast with a swing from 77-133 bar. The bulk volume average pressure is the geomechanical relevant pressure which also takes the response of the aquifers into account. It is defined as  $p_{BV} = \frac{\sum_i V_i p_{i,dc}}{\sum_i V_i}$  with  $p_{i,dc}$  the cell depth corrected pressure and  $V_i$  the cell volume. The figure shows that in each gas bearing block the Bulk volume average pressure follows the gas pressure nearly instantaneously for both forecast scenarios. From 2015 onwards, the standard deviation in the depth corrected cell pressure within each block remains smaller than 3 bar. Hence within each block the pressure equilibrates rapidly.

In contrast the Bulk volume average reservoir pressure shows a delay with respect to the reservoir average gas pressure which can mainly be contributed due to a delayed response in the Northern and Western Aquifers. The difference in block pressures over the midfield fault remains smaller than 16 bar during the forecast cycles, similar to the 77-133 bar case.

Compared to the 77-133 bar case the difference between Bulk volume average and gas pressure only slightly increases in terms of magnitude. The time delay in the response of the Bulk volume average pressure is comparable. The maximum injection rate is limited by the pump capacity which is the same as for the 77-133 bar cycles. The maximum rate is only maintained over a longer period in time during the 77-150 bar cycles.

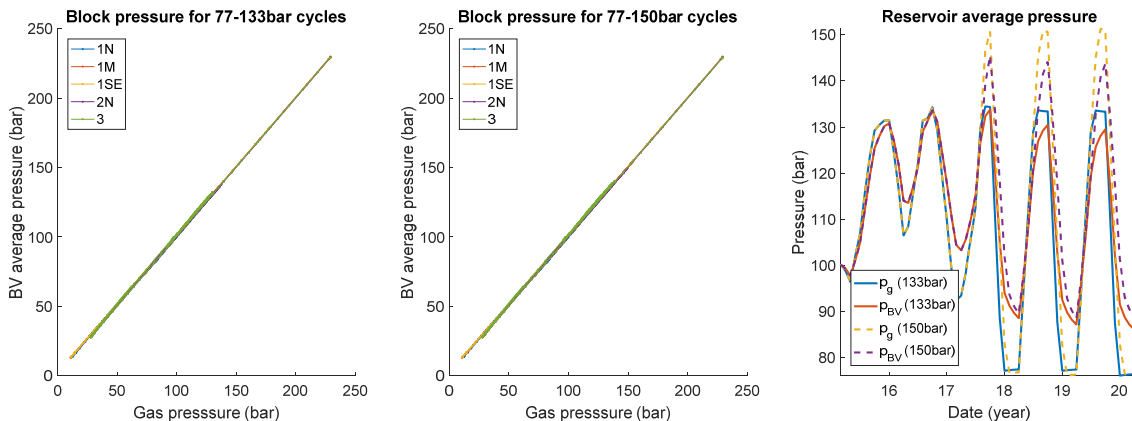


**Figure 1: Bulk Volume average block pressure versus gas block pressure in the gas bearing blocks (left) 77-133 bar forecast cycles and (middle) 77-150 bar forecast cycles. (Right) figure shows the bulk volume average reservoir pressure and gas pressure in time for both forecasts.**

## 3 Stress simulation for 77-150 bar forecast cycles

If the storage capacity of the reservoir is enlarged by increasing the maximum pressure to 150 bar, the forecast cycles will get a larger pressure range. However, the two main factors that determine seismic risk remain unaltered: the lowermost pressure and the rate of pressure increase which is limited by the pump capacity.

### Midfield fault

The time evolution of the stress on the MC diagram remains the same, see Figure 4. The stress cycles have become a bit larger, but towards the stable side. The maximum magnitude in Figure 6 is slightly different, also in the historical simulation. These deviations do not indicate systematic changes in stress (as shown by

Figure 5) but are caused by small numerical deviations in the stress and high sensitivity to these deviations, because the computed critical area and the excess shear stress are both small and the slip correction is very sensitive to the stress distribution. Small differences in stress result from a different time stepping algorithm used for the 133 bar and 150 bar case.

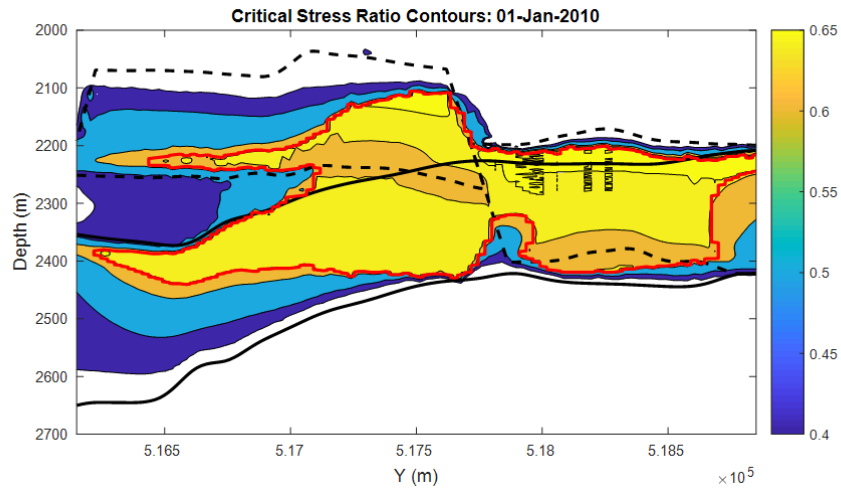


**Figure 2: Contours of critical stress ratio on the Midfield fault, at the start of refill. The black lines indicate the reservoir blocks (solid for Eastern side and dashed for Western side). The red line is the maximum critically stressed area during depletion on which the stress is computed to determine how close the fault is to inducing large earthquakes.**

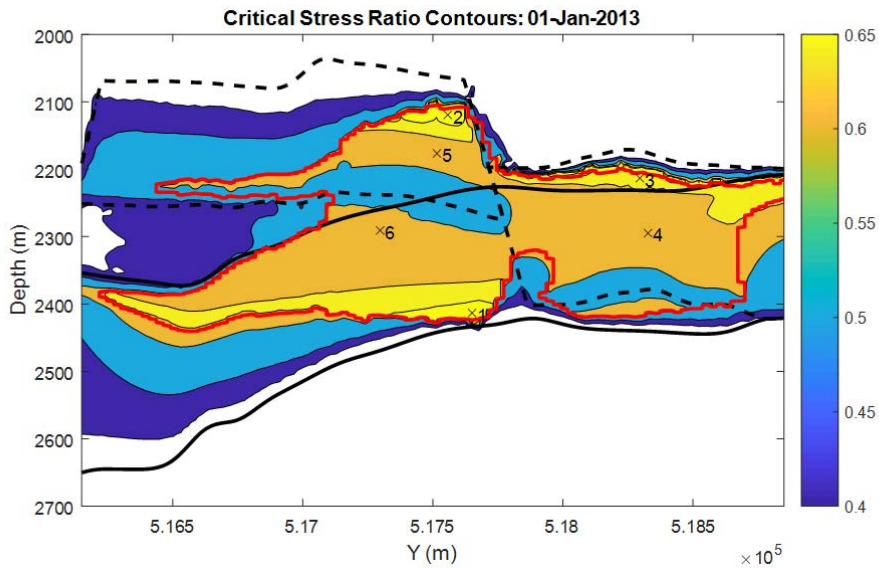


**Figure 3: Contours of critical stress ratio on the Midfield fault, just before the time of the largest micro-seismic event. The only critically stressed patches occur at the boundaries of the maximum slippage area.**

On the Midfield fault, the most critical area responded different to the cycles compared with the average critical stress, since the most critical point was caused by the additional shear stress due to depletion slip. However, cumulative slip on this critically stressed fault patch is a good explanation for disappearance of seismicity. That means that also for larger pressure cycles, this critically stressed area has stabilized so that further pressure increase will not give more seismicity. Figure 5 shows that the first cycle in the forecast still reaches criticality, but that disappears for later cycles. The maximum magnitude plotted in Figure 6 shows that the magnitude is also comparable to the predicted magnitude in the historical cycles.

The seismicity rate (Figure 7) is also similar to the 133 bar case, since the rate of change is dictated by the pump capacity, so is independent of the pressure range. The fluctuations in critical stress ratio ( $R_{c,N}$ ) are a bit larger for the 150 bar case, but the peaks are the same for the same lower bound of the pressure (Figure 6).

*Sensitivity: Seismic risk when no slip correction is applied after depletion*

As sensitivity it assumed that during refill and storage the faults do not slip. Figure 8 shows that this does not increase the seismic risk magnitude significantly compared to the 77-133 bar case, because the increased seismic risk levels off at higher pressure. Hence, the maximum magnitude of 2.2 that is predicted for this worst case is the same as the maximum magnitude for 133 bar maximum pressure. The fluctuations in critical stress ratio ( $R_{c,N}$ ) for micro-heterogeneity are a bit larger for the 150 bar case when compared to the 133 bar case, but the peaks remain unaltered and are obtained at the lower bound of the pressure range.

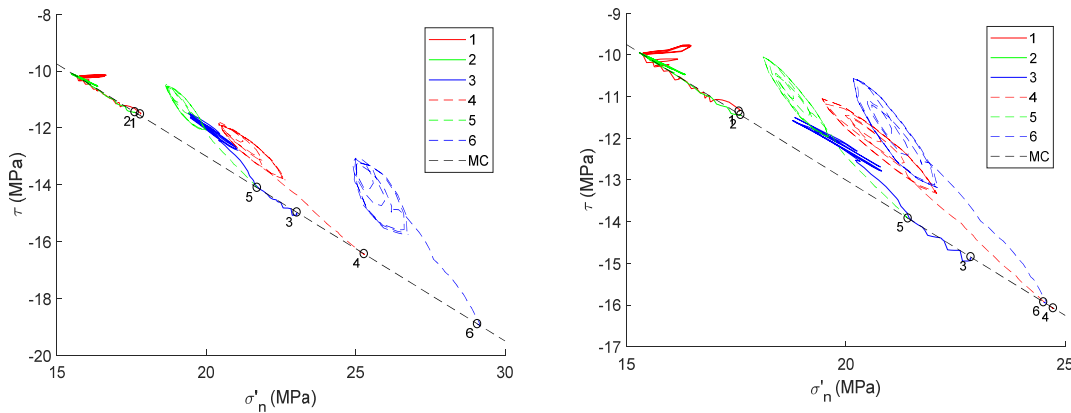


**Figure 4: MC plot of selected points on the fault, shown in Figure 3. (left) 77-133 bar cycles (right) 77-150 bar cycles. Note that the points are chosen at slightly different position (77-133 vs 77-150 bar), this results in slightly different stress paths. However the overall trend is the same (see text).**

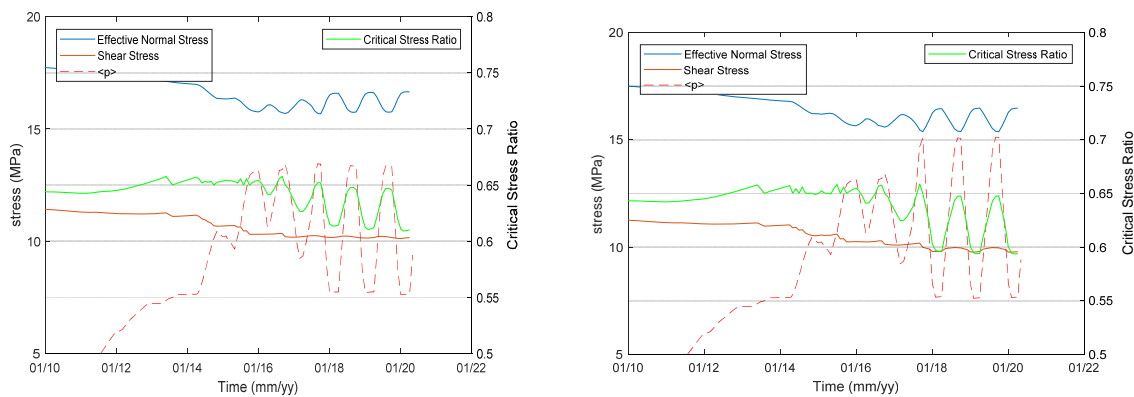


**Figure 5: Normal stress, shear stress and critical stress ratio for point 1 (see Figure 3) vs. time. The critical stress ratio at this peaks at high average reservoir pressure, due to the additional shear stress from the depletion earthquakes. (left) 77-133 bar cycles (right) 77-150 bar cycles.**

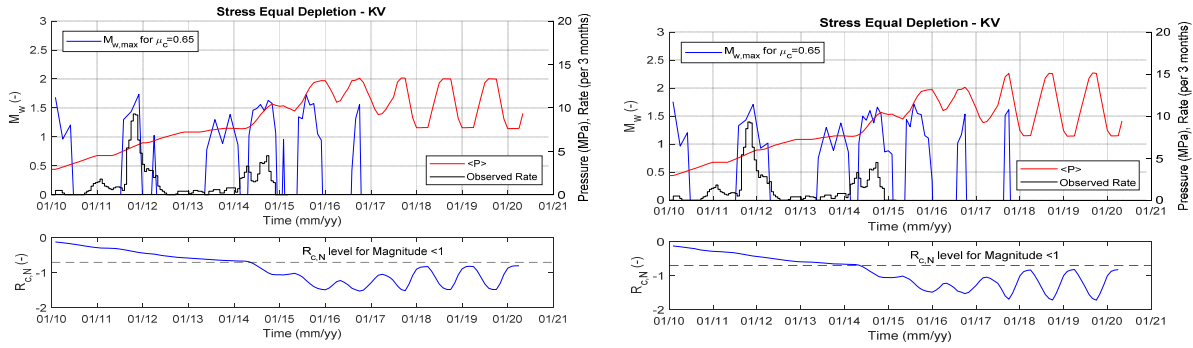


**Figure 6: Magnitude from slip for the Midfield fault with average gas pressure and observed micro-seismic rate (upper graphs) for (left) the 133 bar case (right) the 150 bar case. Rate is defined as events per 3 months times 0.1. The lower graphs show the average critical stress ratio. This ratio remains below the level of the maximum recorded historical micro-seismic event of magnitude 1.**

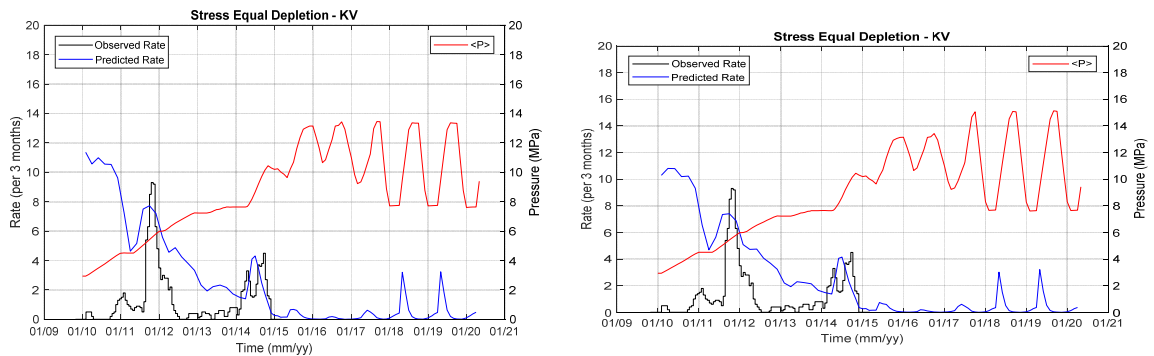


**Figure 7: Micro-seismic rate and predicted rate that is derived from the shear stress rate and the stress level on the fault. Rate is defined as event per 3 months times 0.1. The predicted rate was calibrated on the absence of micro-seismicity after 2014. Refill, storage and (left) 77-133 bar forecast cycles and (right) 77-150 bar forecast cycles.**

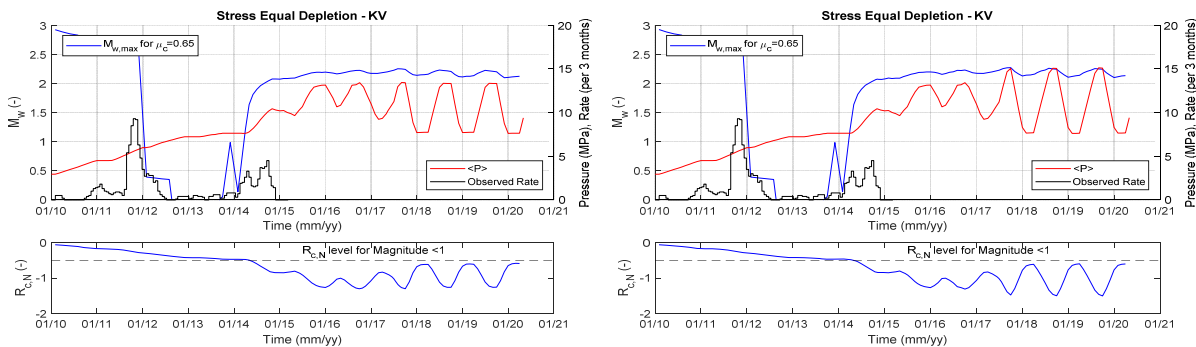


**Figure 8: Magnitude from potential slip for the Midfield fault with average gas pressure and observed micro-seismic rate (upper graphs) for (left) the 133 bar case (right) the 150 bar case with friction coefficient 0.65. Rate is defined as event per 3 months times 0.1. In this case, no slip was applied, so the critically stressed region persists. The maximum magnitude of 2.2 that is predicted for this worst case is the same as the maximum magnitude for 133 bar maximum pressure. The lower graphs show the average critical stress ratio.**

### East Fault 150 bar Case

The stress on the East fault behaves in a normal manner with the most critical point at low pressure. So, the predicted behaviour for 150 bar maximum pressure is the same as was found for 133 bar. The critical stress ratio in Figure 9 is also far below a level that could give strong seismicity and the rate (Figure 10) is also the

same. The increase in predicted seismic rate for the forecast cycles is caused by the faster injection rate during the forecast cycles when compared to the historical cycles. Because the maximum injection rates are the same for the 133 bar and 150 bar cases, the predicted seismic rate is the same for both cases.

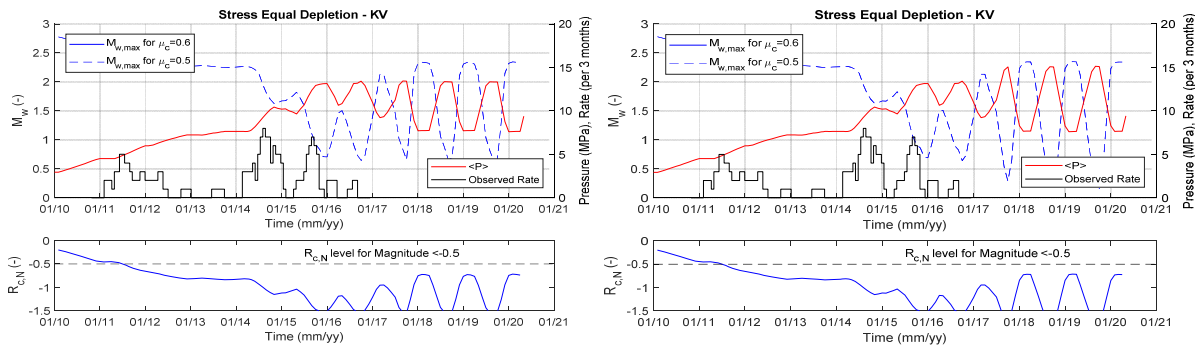


**Figure 9: Magnitude from slip for the East fault with average gas pressure and observed micro-seismic rate (upper graphs) for (left) 77-133 bar case and (right) 77-150 bar case. Rate is defined as events per 3 months. The lower graphs show the average critical stress ratio. During the storage cycles the ratio remains below the level of the maximum recorded historical micro-seismic event in 2011.**

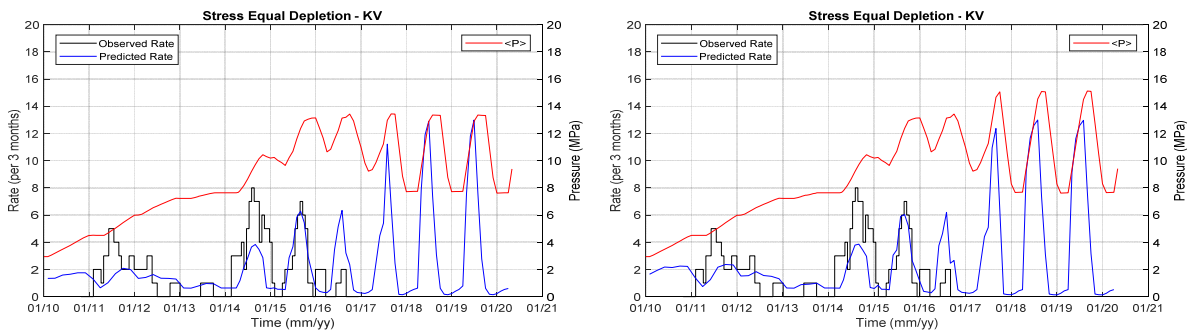


**Figure 10: Micro-seismic rate and predicted rate that is derived from the shear stress rate on the fault. Rate is defined as events per 3 months. (left) 77-133 bar cycles and (right) 77-150 bar cycles.**

## Conclusions

- The most critical patch on the Midfield fault is most unstable at high pressure but the critical stress ratio is about the same for 150 bar compared with 133 bar, because it levels off at higher pressure. Therefore, increasing the working pressure to 150 bar does not increase the seismic risk compared with storage cycles with maximum pressure of 133 bar.
- For the entire fault, seismic risk is determined by the lower pressure bound of the storage cycles, for which the Midfield fault becomes most critical. So, the average critical stress ratio is not affected by the higher working pressure.
- The micro-seismicity rate at the East fault is determined by pressure rate. Since the rate is the same for higher working pressure, the expected seismic rate at the East fault will not increase for higher working pressure.

## 4 Subsidence and Heave for forecast cycles

Figure 11 compares the response in the heave for the forecast run with 77-150 bar swing in comparison to forecast run with a swing of 77-133 bar, using the parameters that were calibrated on the refill and storage heave. Simulation predicts a maximum heave of about 13mm starting from 2014 and a maximum swing of approximately 10mm during the forecast cycles. This gives a small increase in the maximum heave by 2mm compared to the 77-133bar case.

The Kelvin-Voigt fit of the simulation gives a fairly good match. Moreover, the relaxation times belonging to the simulations including the forecast are close to the relaxation time for the historical storage cycles only. The relaxation times are the same as for the 77-133 bar forecast cycles. This confirms again that the pressure equilibrates fast within a domain.

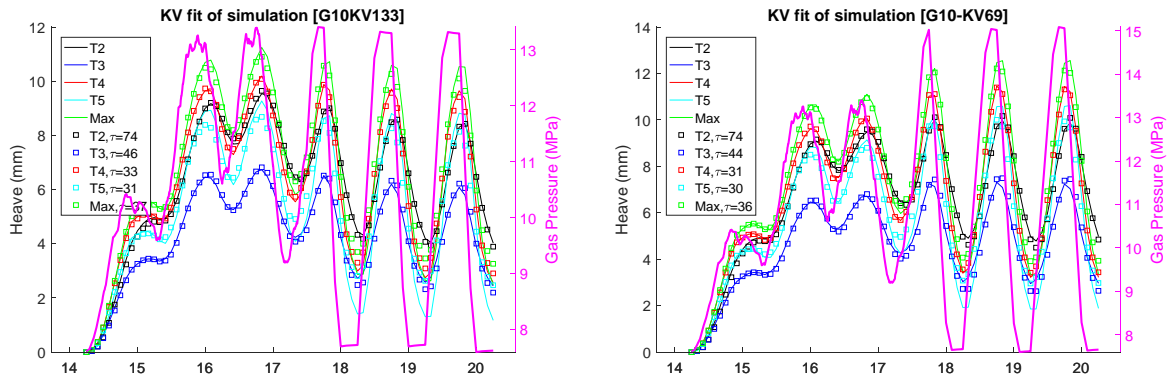


**Figure 11: Response heave of the 4 observation stations and the maximum heave during the historical storage and forecast simulations (2014-2021) plotted against the gas pressure. (left) 77-133 bar forecast cycles and (right) 77-150 bar forecast cycles. The squares are a Kelvin-Voigt fit of the FEM results for which the corresponding relaxation time are shown.**

## 5 Discussion

Overall the Faults stabilize with increasing reservoir pressure analogue to the Kaiser effect, when the effects of differential compaction are reversed. This causes the micro-seismicity to become more pronounced at the low pressures during a storage cycle, while it stabilizes at higher pressures.

The centre of the depletion slip area rapidly moves away from the Mohr-Coulomb failure envelop when the pressure is increased. However, depletion slip results in a shear stress increment at the periphery of the depletion slip area, resulting from the excess shear stress distribution of the area that exceeds the Mohr-Coulomb failure criterion. During pressurization this shear stress increment dominates the nominator of the Mohr-Coulomb failure criterion, such that a reduced effective normal stress destabilizes the edges of the depletion slip area. However, the excess shear stress in these areas remains small such that the magnitude of the seismicity will remain small as well. Moreover, this effect is especially pronounced at the start of the pressurization, while its sensitivity levels off at higher pressures because of the dominance of the overall Kaiser effect. As a consequence, the estimate for the maximum moment magnitude is fairly insensitive to an increase of the working pressure from 133 to 150 bar.